УДК 621.396

SIGNAL DATA TRANSMITTED VIA ATMOSPHERIC COMMUNICATION LINKS WITH FADING CAUSED BY TURBULENT GASEOUS IRREGULAR STRUCTURES

DOI 10.36994/2788-5518-2021-01-01-01[1]

Irit Juwile. School of Electrical and Computer Engineering, Ben-Gurion University, Beer-Sheva, Israel ***iritj@sce.ac.il***

Irina Bronfman. *School of Electrical and Computer Engineering, Ben-Gurion University, Beer-Sheva., Israel* ***..irinamo@ac.sce.ac.il***

Nathan Blaunstein. Dr. habil. Phys., Prof. Ben-Gurion University of the Negev, Beersheba, Israel. *nathan.blaunstein@hotmail.com*

Anatjliy Semenko. *Dr. habil.,Prof. Open International university of Human Development"UKRAINE", Kiev, Ukraine. setel@ukr.net*

Abstract.*In this work, we analyze the effects of turbulent gaseous structures, small-scale, moderate-scale, and large-scale, weak and strong, on signal data, which pass via atmospheric communication links with fading. First of all, we analyze the effects of structure parameter of the refractive index deviations on the index of scintillation of the optical signal passing atmospheric channels with fading. Relations between these parameters are investigated both for conditions of weak gaseous turbulences, moderate and strong turbulences observing experimentally in the middle–latitude troposphere. Analytically and numerically was obtained the relation between signal intensity deviations, called the scintillation index, usually used during analysis of optical atmospheric communication links, and the well-known Rician K-parameter of fast fading, usually used during analysis of radio wireless communication channels. to unify both approached for description of tropospheric optical communication links with fading. Secondly we analyze analytically the effects of troposcattering on intensity loss of and its impact in fast fading phenomena occurring in atmospheric links. Finally, using relation between the fading Rician K-factor and scintillation index, the data stream parameters, such as capacity, spectral efficiency and bit-error-rate (BER) is analyzed for predicting of quality of service accounting for the effects of weak, moderate and strong gaseous turbulent structures filled atmospheric channels with fading.*

Keywords: *turbulence, attenuation, refraction, scintillation index, fast fading, quality of service.*

ПАРАМЕТРИ СИГНАЛУ, ЩО ПЕРЕДАЄТЬСЯ ЧЕРЕЗ АТМОСФЕРУ З ФЕДИНГОМ, ПРИЧИНЕНИМ ТУРБУЛЮЮЧИМИ ГАЗОВИМИ НЕРЕГУЛЬОВАНИМИ СТРУКТУРАМИ

Ірит Джувіле*. Школа електротехніки та обчислювальної техніки, Університет Бен-Гуріона, Беер-Шева, Ізраїль iritj@sce.ac.il*

[1] Irit Juwile, Irina Bronfman, Nathan Blaunstein, Anatjliy Semenko

***Ірина Бронфман**. Школа електротехніки та обчислювальної техніки, Університет Бен-Гуріона, Беер-Шева, Ізраїль ..irinamo @ ac.sce.ac.il*

***Натан Блайнштейн**. Д..ф-м.н,, проф.Університет Бен-Гуріона в Негеві, Беер-Шева, Ізраїль. nathan.blaunstein@hotmail.com*

***Анатолій Семенко**. Д.т.н.,проф. Відкритий міжнародний університет розвитку людини "УКРАЇНА", Київ, Україна. setel@ukr.net*

***Анотація.** У роботі аналізується вплив турбулентних газоподібних структур, дрібних, середньомасштабних та великомасштабних, слабких та сильних, на параметри сигналу, який проходить через атмосферні канали з загасанням. Перш за все, аналізується вплив структурного параметра відхилень показника заломлення на показник сцинтиляції оптичного сигналу, що проходить через атмосферні канали із загасанням. Зв'язок між цими параметрами досліджується як для умов слабких газових турбулентностей, помірних, так і сильних турбулентностей, що спостерігаються експериментально в тропосфері середніх широт. Аналітично та чисельно отримано співвідношення між відхиленнями інтенсивності сигналу, званими індексом сцинтиляції, що зазвичай використовуються під час аналізу оптичних зв'язків в атмосфері , та добре відомим K-параметром Rician швидкого завмирання , який зазвичай використовується під час аналізу безпроводових каналів радіозв'язку для уніфікації обох підходів для опису тропосферних оптичних зв'язків із завмиранням. По-друге, аналізуються аналітично ефекти розсіяння на втрату інтенсивності та його вплив на явища швидкого завмирання , що відбуваються в атмосферних каналах. Нарешті, використовуючи співвідношення між коефіцієнтом зменшення коефіцієнта Rician та сцинтиляційним індексом, аналізуються параметри потоку даних, такі як ємність, спектральна ефективність та коефіцієнт похибок бітів (BER) для прогнозування якості обслуговування, враховуючи наслідки слабких, помірних та сильних газоподібних турбулентних структури.*

***Ключові слова** :турбулентність,загасання,заломлення,індекс сцинтиляції, швидке завмирання,якість обслкглвування.*

ПАРАМЕТРЫ СИГНАЛА, ПЕРЕДАВАЕМОГО ЧЕРЕЗ АТМОСФЕРУ С ФЕДИНГОМ, ПРИЧИНЕННЫМ ТУРБУЛЮЮЧИМИ ГАЗОВЫМИ НЕРЕГУЛИРОВАНЫМИ СТРУКТУРАМИ

***Ирит Джувиле.** Школа электротехники и вычислительной техники, Университет Бен-Гуриона, Беэр-Шева, Израиль iritj@sce.ac.il*

***Ирина Бронфман**. Школа электротехники и вычислительной техники, Университет Бен-Гуриона, Беэр-Шева, Израиль ..irinamo @ ac.sce.ac.il*

***Натан Блайнштейн**. Д..ф-м.н ,, проф, Университет Бен-Гуриона в Негеве, Беэр-Шева, Израиль. nathan.blaunstein@hotmail.com*

***Анатолий Семенко**. Д.т.н., проф. Открытый международный университет развития человека "УКРАИНА", Киев, Украина. setel@ukr.net*

***Аннотация.** В работе анализируется влияние турбулентных газообразных структур, мелких, среднемасштабные и крупномасштабных, слабых и сильных, на сигнал,которій проходит через атмосферные каналы с затуханием. Прежде всего,*

анализируется влияние структурного параметра отклонений показателя преломления на показатель сцинтилляции оптического сигнала, проходящего через атмосферные каналы с затуханием. Связь между этими параметрами исследуется как для условий слабых газовых турбулентностей, умеренных, так и сильной турбулентности, наблюдаемые экспериментально в тропосфере средних широт. Аналитически и численно получено соотношение между отклонениями интенсивности сигнала, называемыми индексом сцинтилляции, обычно используемого при анализе оптических связей в атмосфере, и хорошо известным K-параметром Rician быстрого замирания, который обычно используется при анализе беспроводных каналов радиосвязи для унификации обоих подходов для описания тропосферных оптических связей с замиранием. Во-вторых, анализируются аналитически эффектывлияния рассеяния на потерю интенсивности и его влияние на явления быстрого замирания, происходящие в атмосферных каналах. Наконец, используя соотношение между коэффициентом уменьшения коэффициента Rician и сцинтилляционным индексом, анализируются параметры потока данных, такие как емкость, спектральная эффективность и коэффициент ошибок бит (BER) для прогнозирования качества обслуживания, учитывая последствия слабых, умеренных и сильных газообразных турбулентных структур.

Ключевые слова: *турбулентность, затухание, преломление, индекс сцинтилляции, быстрое замирание, качество обслуживания.*

Turbulence Phenomena Background

The temperature and humidity fluctuations combined with turbulent mixing by wind and convection induce random changes in the air density create optical eddies in form of optical turbulence, which is one of the most significant parameters for optical wave propagation in land-atmosphere communication links [1-15]. In other words, atmospheric turbulence is a chaotic phenomenon created by random temperature, wind magnitude variation, and direction variation in the propagation medium. This chaotic behavior results in index-of-refraction fluctuations. Causing a random space-time redistribution of the refractive index in the gaseous layered atmosphere, turbulences cause a variety of effects on an optical wave related to its temporal irradiance fluctuations (called *scintillations* [6-10]) and phase fluctuations. A statistical approach is usually used to describe both atmospheric turbulence and its various effects on visual optic or infrared (IR) rays passing atmospheric links [11-15].

According to classical concepts, the turbulence spectrum is divided into three regions by two scale sizes [1-14]:

* the outer scale (or macro size) of turbulence: L_0;
* the inner scale (or micro size) of turbulence: l_0.

These values vary according to atmosphere conditions, distance from the ground, and other factors. The inner scale l_0 is assumed to lie in the range of 1mm to 30mm. Near ground it is typically observed to be around 3 to 10 mm, but generally increases to several centimeters with increasing altitude h [12-15]. Near ground, the outer scale L_0, is usually taken to be roughly kh, where k is a constant on the order of unity and h is the atmospheric layer of turbulence localization [14, 15]. Thus, L_0

is usually either equal to the height from the ground (when the turbulent cell is close to the ground) or in the range of 10 m to100 m or more. Vertical profile models for the outer scale have been developed based on measurements, but different models predict very different results (see. for example, [6-10]).

Let us outline several aspects from classical analysis of physical properties of turbulent liquid, from which all main postulates were converted to the atmospheric turbulence behavior explanation. Thus, at the earliest study of turbulent flow, Reynolds used theory "of similarity" to define a non-dimensional quantity $Re = V \cdot l/\nu$, called the Reynolds number [1-5], where *V* and *l* are the characteristic velocity (in m/s) and size (in m) of the liquid flow, respectively, and *v* is the kinematic viscosity (in m^2/s).

The transition from laminar to turbulent motion takes place at a critical Reynolds number, above which the motion is considered to be turbulent. The kinematic viscosity *v* of air is roughly 10^{-5} m^2s^{-1} [5-7], then air motion is considered highly turbulent in the in the boundary layer and troposphere, where the Reynolds numbers Re ~ 10^5 [1-5].

Richardson [2] first developed a theory of the turbulent energy redistribution in the atmosphere - the energy cascade theory. It was noticed that smaller-scale motions originated as a result of the instability of larger ones. A cascade process, shown in Fig. 1 rearranged from [22], in which eddies of the largest size are broken into smaller and smaller ones, continues down to scales in which the dissipation mechanism turns the kinetic energy of motion into heat.

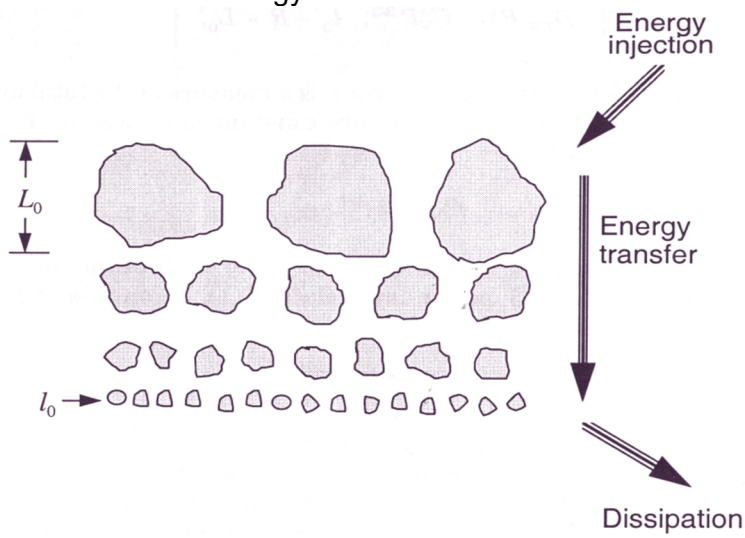

Fig. 1. Richardson's cascade theory of turbulence.

Let us denote by *l* the current size of turbulent eddies, by $L_0$and l_0 - their outer and inner scales, and by:

$$\kappa_0 = \frac{2\pi}{L_0}, \quad \kappa = \frac{2\pi}{l} \text{ and } \quad \kappa_m = \frac{2\pi}{l_0} \tag{1.1}$$

the spatial wave numbers these kinds of eddies, respectively. In this notations, one can divide turbulences at the three regions:

$$\begin{aligned} &\text{Input range } L_0 \le l,\ \kappa < \frac{2\pi}{L_0} \\ &\text{Inertial range } l_0 < l < L_0, \frac{2\pi}{L_0} < \kappa < \frac{2\pi}{l_0} \\ &\text{Dissipation range: } l \ge l_0, \frac{2\pi}{l_0} \ge \kappa \end{aligned} \tag{1.2}$$

These three regions induce strong, moderate, and weak spatial and temporal variations, respectively, of signal amplitude and phase, referred to in the literature as *scintillations* [4-6, 10, 14].

Kolmogorov [1] introduced a hypothesis stating that during the cascade process the direct influence of larger eddies is lost and smaller eddies tend to have independent properties, universal for all types of turbulent flows. Following Kolmogorov, the energy cascade process consists of an energy:

- input subrange,
- inertial subrange, and
- energy dissipation subrange,

as it is sketched in Fig. 1.

At large characteristic scale or eddy, a portion of kinetic energy in the atmosphere is converted into turbulent energy. When the characteristic scale reaches an outer scale size, L_0, the energy begins a cascade that forms a continuum of eddy size for the energy transfer from a macroscale L_0 to a microscale l_0 called the inner turbulence scale. The scale sizes l bounded above by L_0 and below by l_0 form the inertial sub-range.

Kolmogorov proposed that in the inertial sub-range, where $L_0 > l > l_0$, turbulent motions are both homogeneous and isotropic and energy may be transferred from eddy to eddy without loss, i.e., the amount of energy that is being injected into the largest structure must be equal to the energy that is dissipated as heat [1].

When the size of a decaying eddy reaches l_0, the energy is dissipated as heat through viscosity processes. It was also hypothesized that the motion associated with the small-scale structure l_0 is uniquely determined by the kinematic viscosity v and ε, where $l_0 \sim \eta = (v^3 / \varepsilon)^{1/4}$ is the Kolmogorov microscale, and ε is the average energy dissipation rate [9-14]. The Kolmogorov microscale defines the eddy size dissipating the kinetic energy. The turbulent process, shown schematically in Fig. 1 according to simple theory of Richardson, was then summarized by Kolmogorov and Obukhov (called in the literature Kolmogorov-Obukhov turbulent cascade process [1]) as follows: the average energy dissipation rate ε of the turbulent kinetic energy will be distributed over the spatial wavelength κ - range as [10]:

$$\begin{aligned} &\text{In the input range } (\kappa_0 \sim 1/L_0)\ \varepsilon \sim \kappa_0^{-5/3} \\ &\text{In the inertial range } (\kappa \sim 1/l):\ \varepsilon \sim \kappa^{-5/3} \end{aligned} \tag{1.3}$$

In the dissipation range (κ_m~1/ l_0): ε ~$\kappa_m^{-5/3}$

where, as above, L_0, l, and l_0 are the initial (outer), current and inner turbulent eddy sizes.

In general, turbulent flow in the atmosphere is neither homogeneous nor isotropic. However, it can be considered locally homogeneous and isotropic in small sub-regions of the atmosphere. Finally, we should mention that atmospheric turbulences due to their motion can cause strong frequency-selective or flat fast fading (see [15]). Below, in Section 2, we will analyze briefly optical signal intensity scintillation phenomenon of passing the atmospheric channel filled by turbulent structures – from small to large. Section 3 will illustrate results of tropospheric scattering of optical signal occurring in the turbulent atmosphere. In Section 4, the effects of atmosphere turbulences on optical signal fading occurring in the optical wireless link. Finally, Section 5 will illustrate of how turbulent structures, which cause fast frequency selective fading and signal intensity scintillations, affect main parameters of information data stream passing such irregular atmospheric channels.

Scintillation of Optical Signals Passing the Turbulent Atmospheric Links

Optical waves, traveling through the turbulent atmosphere, which is characterized by rapid variations of refraction indexes (see previous paragraphs), undergo fast changes in their amplitude and phase [6-15]. This effect is called *dry tropospheric scintillation*. The phase and amplitude fluctuations occur both in the space and time domains. Moreover, this phenomenon is strongly frequency-dependent: the shorter wavelengths lead to more severe fluctuations of signal amplitude and phase resulting from a given scale size [10-15]. The scale size can be determined by experimental monitoring the scintillation of an optical signal on two nearby paths and/or by examination of the cross-correlation between the scintillations along the propagation paths. If the effects are closely correlated, then the scale size is large compared with the path spacing [6, 7]. Additional investigations have shown that the distribution of the signal fluctuations (in decibels) is approximately a Gaussian distribution, whose standard deviation is the intensity [10-15].

A wave propagating through a random medium such as the atmosphere will experience irradiance fluctuations, called scintillations, even over relatively short propagation paths. Scintillation is defined as [10, 13-15]:

$$\sigma_1^2 = \frac{\langle I^2 \rangle - \langle I \rangle^2}{\langle I \rangle^2} = \frac{\langle I^2 \rangle}{\langle I \rangle^2} - 1 \qquad (2.1)$$

This is caused almost exclusively by small temperature variations in the random medium, resulting in index-of-refraction fluctuations (i.e. turbulent structures). In (2.1) the quantity I denotes irradiance (or intensity) of optical wave and the angle brackets denote an ensemble average or equivalently, a long-time average. In weak fluctuation regimes, defined as those regimes for which the scintillation index is less

than one [2, 10, 13-15], derived expressions for the scintillation index show that it is proportional to Rytov variance:

$$\sigma_1^2 = 1.23 C_n^2 k^{7/6} R^{11/6} \quad (2.2)$$

Here, C_n^2 is the index-of-refraction structure parameter defined in [2, 10-14], $k=2\pi/\square$ is the radio wave number, $\square$ is the wavelength, and R is the propagation path length between transmitter and receiver.

Fig. 2 presents scintillation index as function of the index-of-refraction structure parameter for various optical wavelengths varied from 300 nm (visual optic band) to 30 μm (far infrared band) for optical channels of lengths R ranged from 100 m to 1 km.

Parameter C_n^2 was taken from real experiments observed in the middle-latitudinal tropospheric regions described in [2, 10-14] for weak, moderate and strong variation of the refractive index n.

As follows from illustrations shown by Fig. 2a to Fig.2c, for desired optical communication links of the constant length, the scintillation index (e.g., the standard deviation of the optical signal intensity fluctuations) increases linearly with increase of the structural refraction parameter C_n^2, and the velocity of growth is such linear dependence increases with decrease of optical wavelength – from 30 μm to 300 nm. So, a sensitivity of optical wave in the visual optic band is much higher to the character of turbulence, weak, moderate and strong, defined by parameter C_n^2, with respect to that in infrared optic band.

For the same situation with turbulence filled atmospheric channel, i.e., for C_n^2= const, for every length of the channel, with increase of wavelength of optical wave passing such a channel, deviations of signal intensity become weaker, and for wavelengths exceeding 10 μm, the channel can be considered to be ideal, that is, neither time dispersive non frequency dispersive.

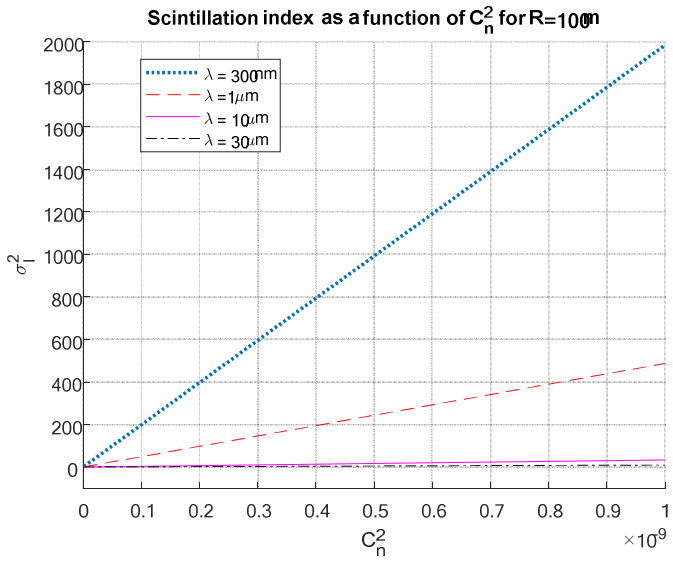

(a)

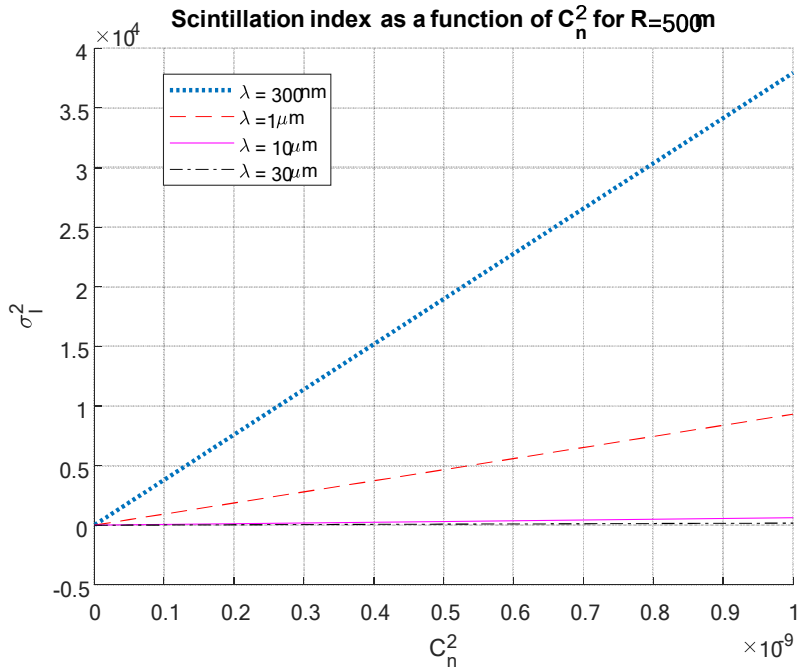

(b)

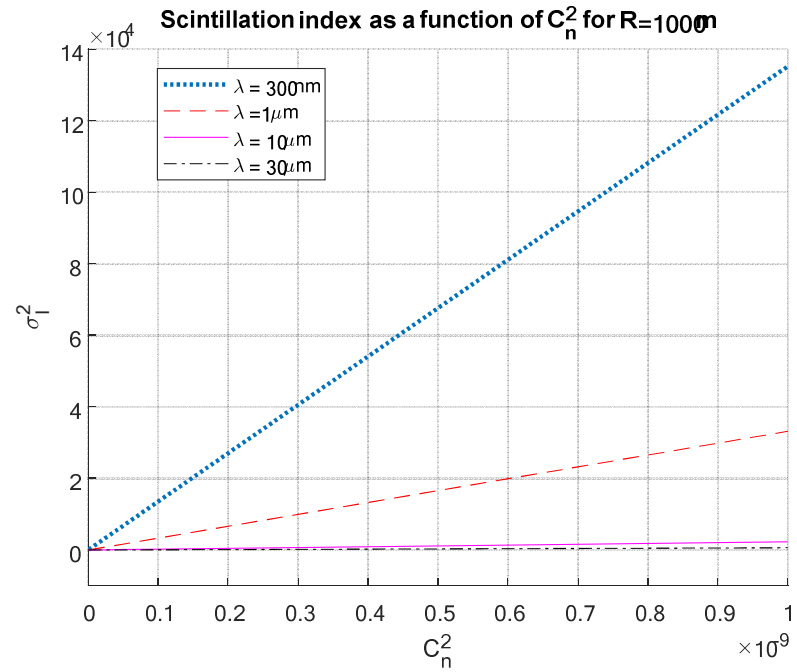

(c)

Fig. 2. Scintillation index as function of the index-of-refraction structure parameter for various optical wavelengths λ for optical channels of lengths R:
(a) R = 100m; (b) R = 5000m; (c) R = 1000m.

Finally for infrared optical waves we can expected a low fading (see below). Moreover, with increase of the length of the atmospheric channel, for constant other parameters of the channel and the signal, the scintillation index can increase per order with increase of the length from 100m to 1km.

The Rytov variance represents the scintillation index of an unbounded plane wave in the case of its weak fluctuations but is otherwise considered a measure of the turbulence strength when extended to strong-fluctuation regimes by increasing either C_n^2 or the path length *R,* or both. It is shown in [2, 10-14] that the scintillation index increases with increasing values of the Rytov variance until it reaches a maximum value greater than unity in the regime characterized by random focusing, because the focusing caused by large-scale inhomogeneities achieves its strongest effect. With increasing path length or inhomogeneity strength, multiple scattering weakens the focusing effect, and the fluctuations slowly begin to decrease, saturating at a level for which the scintillation index approaches the value of one from above. Qualitatively, saturation occurs because multiple scattering causes the optical wave to become increasingly less coherent in the process of wave propagation through random media.

Early investigations concerning the propagation of unbounded plane waves and spherical waves through random media obtained results limited by weak fluctuations [6, 7]. To explain the weak-fluctuation theory, three new parameters of the problem must be introduced instead of the inner and outer scales of turbulences described earlier. They are:

(a) the coherence scale, $l_1 \equiv l_{\text{co}} \sim 1/\rho_0$, which describes the effect of coherence between two neighboring points (see [10, 14]);

(b) the first Fresnel zone scale, $l_2 \equiv \ell_F \sim \sqrt{R/k}$, describes the clearance of the propagation link (see [10, 14]);

(c) the scattering disk scale, $l_3 \sim R/\rho_0 k$, which models the turbulent structure, where *R* is the length of the radio path.

On the basis on such definitions, Tatarskii [2] predicted that the correlation length of the irradiance fluctuations is of the order of the first Fresnel zone $\ell_F \sim \sqrt{L/k}$ (see details in [10, 14]). However, measurements of the irradiance covariance function under strong fluctuation conditions showed that the correlation length decreases with increasing values of the Rytov variance $\sigma_1^2$and that a large residual correlation tail emerges at large separation distances.

In [10, 14], the theory, developed in [6, 7], was modified for strong fluctuations and showed why the smallest scales of irradiance fluctuations persist into the saturation regime. The basic qualitative arguments presented in these works are still valid. Kolmogorov theory assumes that turbulent eddies range in size from a macroscale to a microscale, forming a continuum of decreasing eddy sizes.

The largest eddy-cell size smaller than that at which turbulent energy is injected into a region, defines an effective outer scale of turbulence L_0, which near the ground is roughly comparable with the height of the observation point above ground.

An effective inner scale of turbulence l_0 is associated with the smallest cell size before energy is dissipated into heat.

Here, we will present briefly modifications of the Rytov method obtained in [13-15] to develop a relatively simple model for irradiance fluctuations that is, applicable to moderate-to-strong fluctuation regimes. In [10, 14], the following basic observations and assumptions have been stated:

a) atmospheric turbulence as it pertains to a propagating wave is statistically ihomogeneous;

b) the received irradiance of a wave can be modeled as a modulation process in which small-scale (diffractive) fluctuations are multiplicatively modulated by large scale (refractive) fluctuations;

c) small-scale processes and large-scale processes are statistically independent;

d) the Rytov method for signal intensity scintillation is valid even in the saturation regime with the introduction of a spatial frequency filter to account properly for the loss of spatial coherence of the wave in strong-fluctuation regimes;

e) the geometrical-optics method can be applied to large-scale irradiance fluctuations.

These observations and assumptions are based on recognizing that the distribution of refractive power among the turbulent eddy cells of a random medium is described by an inverse power of the physical size of the cell. Thus, the large turbulent cells act as *refractive lenses* with focal lengths typically on the order of hundreds of meters or more, creating the so-called *focusing effect* or *refractive scattering*.

This kind of scattering is defined by the coherent component of the total signal passing the troposphere. The smallest cells have the weakest refractive power and the largest cells the strongest. As a coherent wave begins to propagate into a random atmosphere, the wave is scattered by the smallest of the turbulent cells (on the order of millimeters) creating the so-called *defocusing effect* or *diffractive scattering*. This kind of scattering is defined by the incoherent component of the total signal. Thus, they act as defocusing lenses, decreasing the amplitude of the wave by a significant amount, even for short propagation distances.

As was shown in [22-24], in the strong-fluctuation regime, the spatial coherence radius ρ_0 of the wave determines the correlation length of irradiance fluctuations, and the scattering disk characterizes the width of the residual tail:$R/\rho_0 k$.

The diffractive scattering spreads the wave as it propagates. Refractive and diffractive scattering processes are compound mechanisms, and the total scattering process acts like a modulation of small-scale fluctuations by large-scale fluctuations. Schematically such a situation is sketched in Fig. 3 containing both components of the total field. Small-scale contributions to scintillation are associated with turbulent cells smaller than the Fresnel zone $\sqrt{R/k}$ or the coherence radius ρ_0, whichever is smaller.

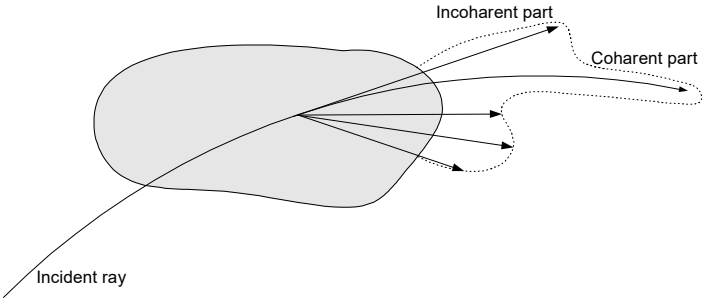

Fig. 3. Optical wave intensity pattern consisting of the coherent part (I_{co}) and incoherent part (I_{inc}).

Large-scale fluctuations in the irradiance are generated by turbulent cells larger than that of the first Fresnel zone or the scattering disk $x/k\rho_0$, whichever is larger, and can be described by the method of geometrical optics. Under strong-fluctuation conditions, spatial cells having size between those of the coherence radius and the scattering disk contribute little to scintillation.

Hence, because of the loss of spatial coherence, only the very largest cells nearer the transmitter have focusing effect on the illumination of small diffractive cells near the receiver. Eventually, even these large cells cannot focus or defocus. When this loss of coherence happens, the illumination of the small cells is (statistically) evenly distributed and the fluctuations of the propagating wave are due to random interference of a large number of diffraction scattering of the small eddy cells.

Optical Signals Tropospheric Scattering

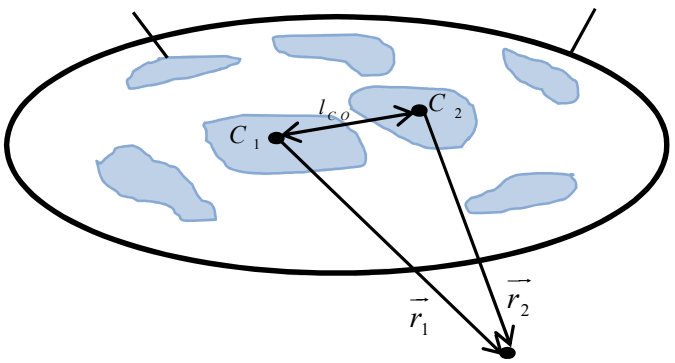

Fig. 4. The coherency between two neighboring points, described by correlation scale lco.

For optical rays passing through the atmosphere, the dominant propagation mechanism is the scattering from atmospheric turbulent eddies and discontinuities in the refractive index of the atmosphere. For the troposcattering optical rays' propagation the received signals are generally 30 to 50 dB below free space values and are characterized by short-term fluctuations superimposed on long-term

variations [10, 14, 15]. Let us briefly consider a problem of optical wave propagation in the turbulent atmospheric gaseous environment, where each turbulent eddy is randomly distributed, as follows from Fig. 4.

The coherency between two neighboring points, can be described by the coherent function of fluctuations of the refractive coefficient □*n*(**r**) of the environment in two points *C*1 and C_2 (see Fig. 4), as:

$$B_n(l_{co}) = \langle \delta n(\boldsymbol{r}_1, t) - \delta n(\boldsymbol{r}_2, t) \rangle \quad (3.1)$$

Here the angular brackets mean ensemble averaging. From classical theory of turbulence, it follows that the correlation function linearly depends on standard deviation of refractive index, σ_n, and exponentially - on relations between the range of the neighboring points, l_{co}, and the current size of the turbulent eddies, *l*, which, as follows from (1.1), lies between their inner $l_0$and outer L_0 scales, that is:

$$B_n(\rho) = \sigma_n^2 exp\{-{l_{co}}^2/l^2\} \quad (3.2)$$

Accounting for the atmospheric turbulent gas as a quasi-homogeneous and quasi-stationary environment (in the case when turbulent gas moves across the receiver in time larger than the time of deviations of the refractive index), let us introduce the coordinates of the "differential" point ***r*** between two neighboring points location, and the "central" point ***R*** of the tested area where receiver is located, respectively:

$$\boldsymbol{r} = \boldsymbol{r}_1 - \boldsymbol{r}_2\,, \quad \boldsymbol{R} = (\boldsymbol{r}_1 + \boldsymbol{r}_2)/2 \quad (3.3)$$

Usually, instead of the refractive index n, the permittivity of the turbulent gas □ is used, as a main parameter describing fluctuation of the medium inside the propagation link, because the normalized (to that in free space) permittivity □□□0□□□□*n*^{2}, □0 is the dielectric constant of vacuum. If so, the correlation function of the permittivity fluctuates can be described similarly, as (3.1):

$$B_\varepsilon(l_{co}) = \langle \delta\varepsilon(\boldsymbol{r}_1) - \delta\varepsilon(\boldsymbol{r}_2) \rangle \quad (3.4)$$

Our problem is to find at the receiver the spectrum of locally homogeneous turbulent permittivity fluctuations at the distance ***R*** from its center, defined by the spectral function of turbulent gas permittivity spatial fluctuations, $\Phi_\varepsilon(\boldsymbol{K}, \boldsymbol{R})$. For this purpose, we should account for the relation between the spectrum $\Phi_\varepsilon(\boldsymbol{K}, \boldsymbol{R})$ and the above correlation function defined by (3.4) via the Fourier transform:

$$\Phi_\varepsilon(\boldsymbol{K}, \boldsymbol{R}) = (2\pi)^{-3} \int d\boldsymbol{r}\, exp(-i\boldsymbol{K}\cdot\boldsymbol{r})\, B_\varepsilon(\boldsymbol{r}, \boldsymbol{R}) \quad (3.5)$$

The expression for the effective scattering volume has the form [15-17]:

$$V_e = \int d\boldsymbol{R}\, F(\boldsymbol{n}_i, \boldsymbol{n}_s)\ \Phi_\varepsilon(\boldsymbol{K}, \boldsymbol{R})/\Phi_\varepsilon(\boldsymbol{K}, 0) \quad (3.6)$$

where:

$$F(\boldsymbol{n}_i, \boldsymbol{n}_s) = |f_i(\boldsymbol{n}_i)\ f_s(\boldsymbol{n}_s)|^2 \quad (3.7)$$

$f_i(\boldsymbol{n}_i)$ and $f_s(\boldsymbol{n}_s)$ are the radiation patterns of the transmitting and receiving devices, respectively. In (3.6), the spatial wave vector ***K*** is defined as:

$$\boldsymbol{K} = k(\boldsymbol{n}_i - \boldsymbol{n}_s) \quad (3.8)$$

where the unit vectors $\boldsymbol{n}_i = \boldsymbol{r}_i/r_i$ and $\boldsymbol{n}_s = \boldsymbol{r}_s/r_s$ are related to the lines connecting the transmitting and receiving devices (let say, laser and photodetector, respectively) with the center of the scattering volume.

As was shown in [10, 13-15], the average signal intensity of the scattered signal at the receiver is depends on the effective scattered volume and on spectrum at the central point $\boldsymbol{R} = 0$, i.e., on $\Phi_\varepsilon(\boldsymbol{K}, 0)$:

$$I_s = \frac{\pi}{2} k^4 \Phi_\varepsilon(\boldsymbol{K}, 0)\, V_e / r_i^2 r_s^2 \tag{3.9}$$

where $k = 2\pi/\lambda$ is the wave number, r_i is the distance from the optical transmitter to the scattering volume, r_s is the distance from the scattering volume to the optical receiver, V_e is the effective volume of scattering, $\Phi_\varepsilon(\boldsymbol{K}, 0)$ is the spectrum of locally homogeneous turbulent permittivity fluctuations at the center of the turbulent zone. At the receiver, it should be defined the spectrum of locally homogeneous turbulent permittivity fluctuations at the distance $\boldsymbol{R}$ from its center $\Phi_\varepsilon(\boldsymbol{K}, \boldsymbol{R})$.

By using (3.9) for the intensity of the scattered wave, we can calculate the power received by the optical detector as:

$$P_2 = F_s^2 G_2 P_1 \tag{3.10}$$

where *G*2 is the gain of the detector, *P*1 is the power of the optical source (e.g., the transmitter) and the scattering loss is given by [2, 10-14]:

$$F_s^2 = \frac{\pi^2}{2} k^2 \Phi_\varepsilon(\boldsymbol{K}, 0)\, V_e / r_i^2 r_s^2 \tag{3.11}$$

There are two unknown factors in Eq. (3.11). The first is the spectrum of signal permittivity deviations, $\Phi_\varepsilon(\boldsymbol{K}, 0)$, which is proportional to the structure parameter of the turbulence. The latter is characterized by a significant variability depending of the structure of turbulences, small-scale, moderate-scale, and large scale [according to definition (1.2)], filled the propagation channel along the optical path. The anisotropic structure of the permittivity fluctuations (or refractive index fluctuations) can also cause rather strong variations of the received power. Indeed, as shown in [10-14], the spectrum $\Phi_\varepsilon(\boldsymbol{K}, 0)$ is strongly depended on dimension *l* of turbulent structure, which we analyzed accounting the polynomial dependence of the structure function of turbulent gas [1, 2, 10-14]. Such polynomial dependence allows to present $\Phi_\varepsilon(\boldsymbol{K}, 0)$ as :

$$\Phi_\varepsilon(\boldsymbol{K}, 0) = 0.033 C_n^2 \left(K^2 + \frac{1}{L_0^2} \right)^{-\frac{11}{6}} \sim K^{-p/2} \tag{3.12}$$

since *K*0 = 2π/*L*0, with the degree *p* of refractive index fluctuations, showing effects of weak small (*p*' = *p*/2= = 1.5÷1.8), moderate (*p*' ~ 1.9÷2.5) and strong large (*p*' ~ 2.5÷3.0) turbulences on optical wave propagation via the atmospheric communication link obtained experimentally at the middle-latitude tropospheric links [10-14]. Indeed, accounting to the Kolmogorov's spectral law with $\Phi_\varepsilon(\boldsymbol{K}, 0) \sim K^{-11/3}$ ~ (for weak turbulences), we get finally that *p*' = *p*/2=5/3 ~ 1.75, which lies inside the range of 1.5÷1.9, and fully coincides to numerous experimental observations carried out at the middle-latitude optical atmospheric links. As for the current dimension of turbulence, *l*, it changes at the range: $1/L_0 < 1/l < 1/l_0$. where the

outer turbulence scale L_0, defined by (1.2) is changed from 500 m to 1300 m, and the inner turbulent scale defined by (1.2) is changed from 1cm to 2 cm [10-14] The computed dependence of signal phase fluctuation spectrum versus the scale of current turbulent structure *l* is shown in Fig. 5.

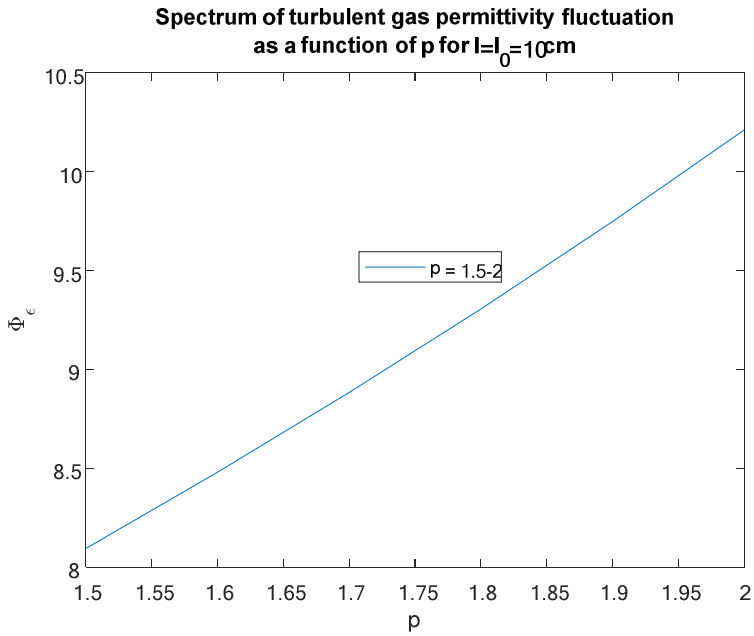

(a)

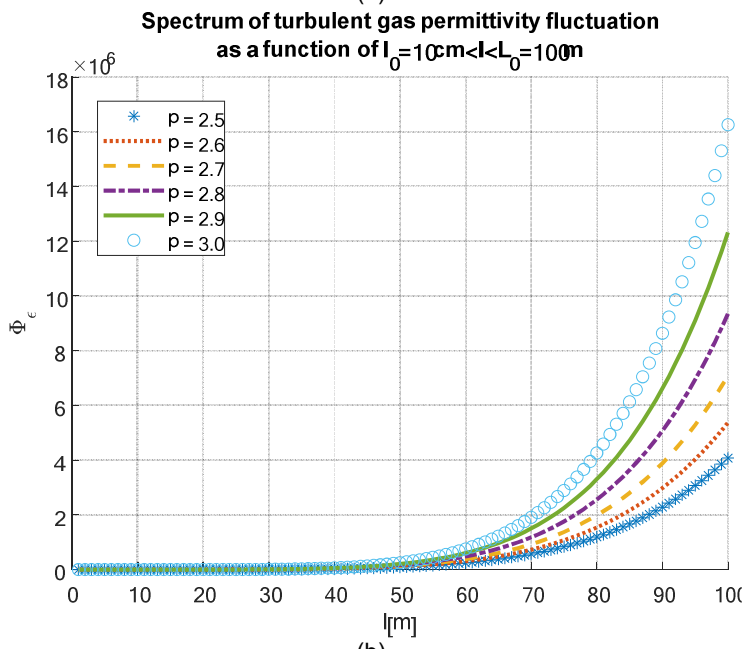

(b)

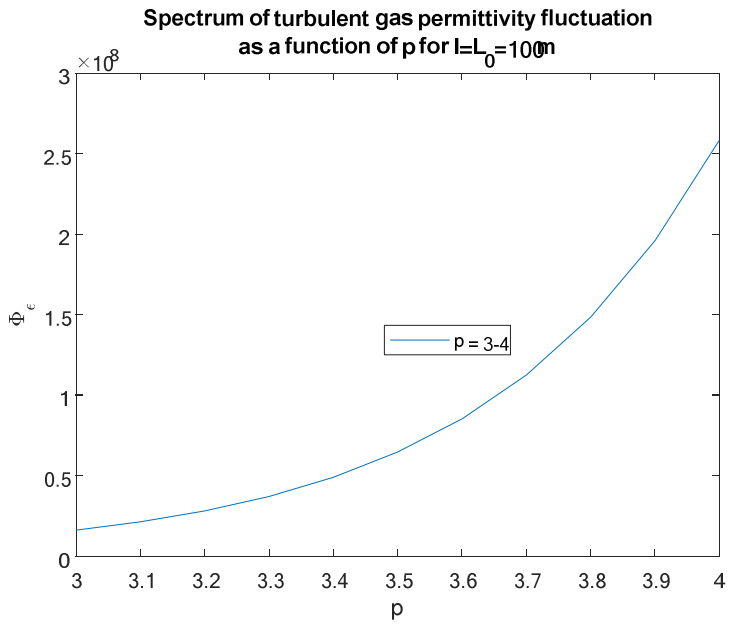

(c)

Fig. 5. Spectrum of turbulent gas permittivity fluctuation as a function of ***K*** for dimension of turbulence, *l*, and degree of phase fluctuations, *p'*: (a) $l = l_0$ = 10cm, *p'* = 1.5-2; (b) l_0 = 10cm< $l < L_0$ = 100m, *p'* = 2.5-3; (c) $l = L_0$ = 100m, *p'* = 3.5-4.

As follows from Figs. 5a-c, with increase of degree of atmospheric gas turbalization – from weak (with *p'* = 1.5-2) to strong (with *p* = 3.5-4) via moderate (with *p'*=2.5-3), spectrum $\Phi_\varepsilon(\boldsymbol{K}, 0)$ and according to Eq. (3.12), the signal scattering loss caused by scattering of optical wave, passing an atmospheric channel filled by various turbulent structures, can essentially increase – from 10^6 to 10^8, that is, in two order, being enough strong. The second factor, affecting the signal scattering loss, is the effective scattering volume V_e , which, according to (3.6)-(3.7), depends essentially on the radiation patterns $f_i(\boldsymbol{n}_i)$ and $f_s(\boldsymbol{n}_s)$ of both optical apertures – of the source of radiation and of the detector, as the receiving device, respectively. Moreover, for sources with relatively small amplification, such those located at the air vehicle (e.g., helicopter), expression (3.6) for the effective scattering volume V_e is no longer valid and should be corrected [10-14].

It is important to outline, that the frequency selectivity of the atmospheric channels is formed by the tropospheric scattering from moving turbulences and leads to the frequency selective fast fading (as will be shown below). Therefore, to complete the evaluation of the link budget and frequency selectivity for the atmospheric optical paths, the realistic models of the atmospheric turbulence, including anisotropic layered structures, as well as the real radiation patterns of the laser beam should be taken into account by use the geometry of optical trace and formulas (3.5) - (3.12) obtained theoretically and presented above.

Effects of Atmosphere Turbulence on Signal Fading

The fast fading of the signal at open paths is caused mainly by multipath propagation and turbulent fluctuations of the refractive index. Some very interesting ideas were proposed in [1, 2, 10], which are presented briefly below. As it is known, the fluctuations of the signal intensity due to turbulence are distributed according to the lognormal law. For the Kolmogorov model, the normalized standard deviation of this distribution can be presented in terms of C_n^2instead of Rytov's formula (2.2) presented now in terms of C_ε^2 :

$$\sigma^2 = 0.12 C_\varepsilon^2 k^{7/6} d^{11/6} \tag{4.1}$$

where $k = 2\pi/\lambda$ is the wave number, and C_ε^2 is the structure constant of the turbulence averaged over the path (sign ε sometimes instead of *n*, because the dielectric permittivity and the refractive index are related as $n^2 = \varepsilon_r$, see [6-9, 15]). In the atmosphere, the structure constant C_ε^2 may vary within at least four orders of magnitude, from 10^{-15} to $10^{-10}\ m^{-2/3}$.

As the path-averaged statistics of these variations is unknown, the margin related to this kind of fading may be estimated only heuristically. The normalized temporal correlation function was obtained in [6-10]:

$$K(\tau) = \frac{1}{sin(\pi/12)}\left[(1+\alpha^4/4)^{11/12}\, sin\left(\frac{\pi}{12} + \frac{11}{6} arctan\frac{\alpha^2}{2}\right) - \frac{11}{6}\left(\frac{\alpha}{\sqrt{2}}\right)^{5/3}\right] \tag{4.2}$$

where $\alpha = \tau/\tau_0$, $\tau_0 = \frac{\sqrt{d/k}}{v}$, and *v* is the projection of the vehicle velocity to the plane that is perpendicular to the path. The correlation time τ_c defined as $K(\tau_c) = 0.5$, can be estimated as $\tau_c \approx 0.62\ \tau_0$. The spectrum of the intensity fluctuations is [6-9]:

$$S(\omega) = \beta^2\, w(\omega)/\omega \tag{4.3}$$

is calculated by using the notion of the normalized spectral density:

$$w(\omega) = 4\omega \int_0^\infty d\tau\, cos(\omega\tau)\, K(\tau) \tag{4.4}$$

which at high and low frequencies is given, respectively by:

$$w(\Omega) = 12.0\ \Omega^{-5/3}, \quad \Omega \geq 5 \tag{4.5a}$$

and at low frequencies can be approximated as:

$$w(\Omega) = 3.47\ \Omega\, exp\left[-0.44\Omega^{\phi(\Omega)}\right]\ \Omega \leq 5 \tag{4.5b}$$

where:

$$\phi(\Omega) = 1.47 - 0.054\ \Omega \tag{4.6}$$

$$\Omega = \tau_0 \omega \tag{4.7}$$

is the dimensionless frequency. The normalized density $w(\Omega)$ has the maximal value of about 2.30 at $\Omega_m \approx 1.60$, and therefore $\omega_m \approx 1.60/\tau_0$ [6-9]. The phase fluctuations have normal distribution [6-8] with dispersion:

$$\sigma_s^2 = 0.075\ C_\varepsilon^2 k^2 d s_0^{-5/3} \tag{4.8}$$

where $s_0 \sim 2\pi/L_0$, and L_0 is the outer scale of the turbulent spectrum depending on the height and equal to approximately 10-100 m [6-9]. Thus, from experiments

described there, it was estimated refraction index power variations around $10^{-10}m^{-2/3}$ (for strong and large-scale turbulence) and around 10^{-15} $m^{-2/3}$ (for weak and small-scale turbulence), for nocturnal and daily periods [8-10]. Computations of dispersion of phase fluctuations caused by fast fading can be done via knowledge of structure parameter of dielectric permittivity variations, C_ε^2, the optical wavelength (via $k = 2\pi/\lambda$), and taking into account deviations of the outer scale of turbulent structures, $l0 < l < L_0$. The result of such computations is shown in Fig. 6 for communication link lengths d = 200, 500, 1000, 2000 m, L_0=50, 100 m, and for the index C_ε^2 varied in magnitude from 10^{-15} to 10^{-10} $m^{-2/3}$.

Estimations carried out according to [9-11] showed that the phase fluctuations caused by turbulence are negligible under typical atmospheric conditions and even for extremely strong turbulence.

Finishing analytical analysis of the effects of atmospheric turbulence on optical signal scattering and fading and comparing the obtained results with experimental data fully described in [9-13], we can summarize that all effects of tropoiscattering, as well as optical signals fast fading caused by atmospheric turbulences, multipath phenomena due to atmospheric turbulence structures - eddies, should be taken into account in land-atmospheric, or atmospheric-atmospheric optical communication links.

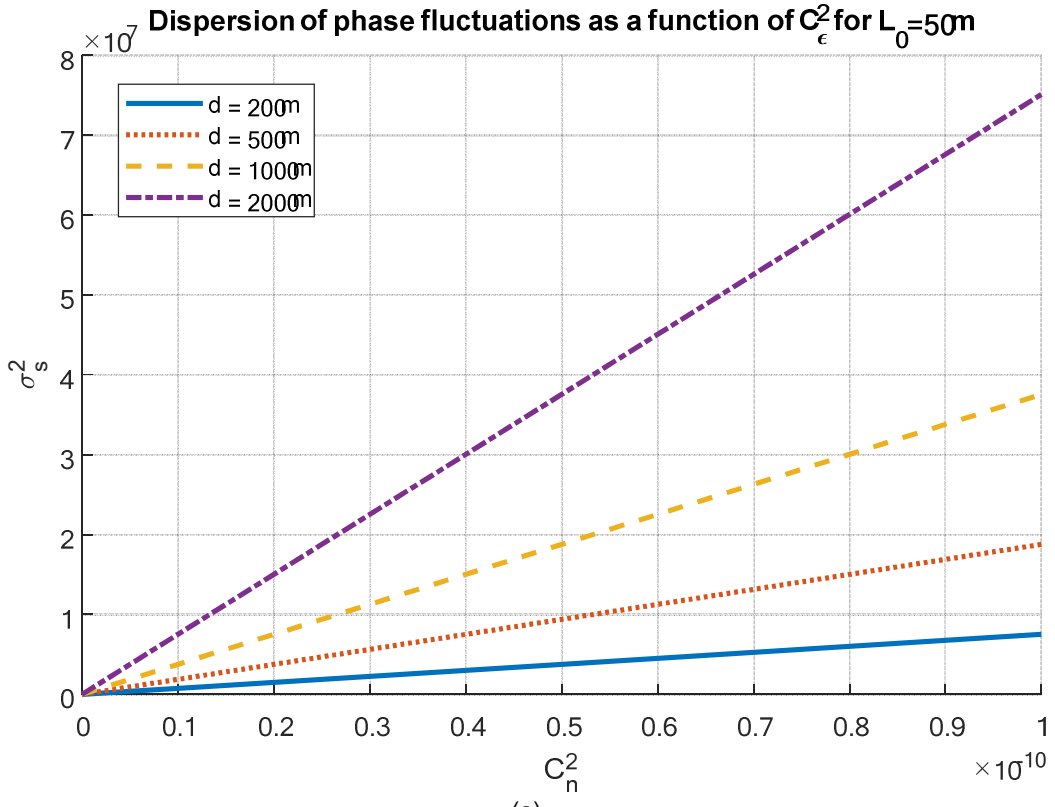

(a)

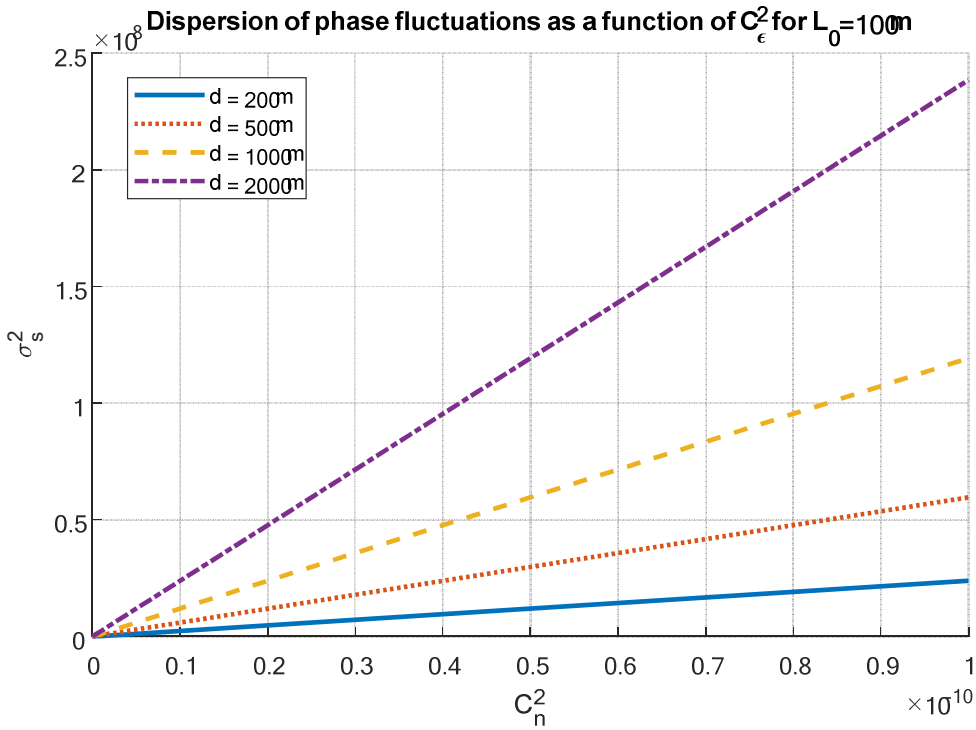

(b)

Fig. 6. Dispersion of phase fluctuations caused by fast fading versus structure parameter of dielectric permittivity variations, C_ε^2, for the optical wavelength $\lambda = 0.5\mu m$ for various communication link lengths, *d,* for the outer scale of the turbulent spectrum L_0: (a) L_0 = 50m; (b) L_0 = 100m.

These effects occurring in the optical atmospheric link formatted its “response” on signal data stream propagation through such kinds of wireless channels with frequency-selective sow and fast fading will be analyzed below by taking into account parameters of data stream, such as capacity and spectral efficiency.

Estimations carried out according to [9-11] showed that the phase fluctuations caused by turbulence are negligible under typical atmospheric conditions and even for extremely strong turbulence.

Finishing analytical analysis of the effects of atmospheric turbulence on optical signal scattering and fading and comparing the obtained results with experimental data fully described in [9-13], we can summarize that all effects of tropoiscattering, as well as optical signals fast fading caused by atmospheric turbulences, multipath phenomena due to atmospheric turbulence structures - eddies, should be taken into account in land-atmospheric, or atmospheric-atmospheric optical communication links. These effects occurring in the optical atmospheric link formatted its “response” on signal data stream propagation through such kinds of wireless channels with frequency-selective sow and fast fading will be analyzed below by taking into account parameters of data stream, such as capacity and spectral efficiency.

Transmission of Information Optical Data Stream via Atmospheric Links

5.1. Main characteristics of information signal data

According to the classical approach, the *capacity* of the AWGN channel of bandwidth $B_\omega$is based on the Shannon-Hartley formula, which defines relation between the maximum data rate via any channel, called the capacity, the bandwidth B_ω [in Hz], and the signal-to-noise ratio (SNR≡ N_{add}) [14, 15]:

$$C = B_\omega \, log_2\left[1 + \frac{S}{N_0 B_\omega}\right] \tag{5.1}$$

where in our notations, the power of additive noise in the AWGN channel is $N_{add} = N_0 B_\omega$, S is the signal power, and $N_0$is the signal power spectrum [in W/Hz].

Usually, in optical communication, other characteristic was introduced, called the *spectral efficiency* of the channel/system [14, 15]:

$$\tilde{C} = \frac{C}{B_\omega} = log_2\left[1 + \frac{S}{N_0 B_\omega}\right] \tag{5.2}$$

Based on the second approach (called the *approximate* [14], accounting for the fading phenomena, flat or multiplicative, we can now estimate the multiplicative noise by introducing a spectral density,N_{mult}, and its frequency bandwidth,B_Ω, in the denominator of the logarithmic function of (5.1), that is:

$$C = B_\omega \, log_2\left[1 + \frac{S}{N_0 B_\omega + N_{mul} B_\Omega}\right] \tag{5.3}$$

where B_Ω is the frequency bandwidth of the multiplicative noise.

Now, as in [14, 15], accounting for $N_{add} = N_0 B_\omega$ and $N_{mult} = N_{mult} B_\Omega$, we can rearrange (5.4) by introducing in it Ricean *K*-factor of fading, defined in [15] as the ratio of the coherent and multipath (incoherent) components of signal intensity, that is, $K = \frac{I_{co}}{I_{inc}}$ (see Fig. 3), or $K = S/N_{mult}$. Using these notations, we finally get the capacity as a function of the *K*-factor and the signal to additive noise ratio:

$$\begin{aligned}(SNR_{add})C &= B_\omega \, log_2\left(1 + \left(SNR_{add}^{-1} + K^{-1}\right)^{-1}\right) \\ &= B_\omega \, log_2\left(1 + \frac{K \cdot SNR_{add}}{K + SNR_{add}}\right)\end{aligned} \tag{5.4}$$

Consequently, it is easy to obtain from (5.3) the spectral efficiency of the channel

$$\tilde{C} = \frac{C}{B_\omega} = log_2\left(1 + \frac{K \cdot SNR_{add}}{K + SNR_{add}}\right) \tag{5.5}$$

where the bandwidth B_ω changes according to the system under investigation. Comparison, made in [14, 15], between the two approaches, classical and approximate, was shown that formulas (5.1) with $N_{add} = N_0 B_\omega$and (5.4), are the same description of the channel/system capacity, when the *K*-factor is larger than SNR_{add}.

Finally, we can relate the strength of the scintillation, introduced in [14-18, 22, 23], which is characterized by the normalized intensity variance, $\langle \sigma_I^2 \rangle$, called the *scintillation index*, with the *K*-factor of fading. In Section 2, we presented this

characteristic for zero-mean random process, following [10-15]. Using mentioned above, we can present formula (2.1) in the following form:

$$\langle \sigma_I^2 \rangle = \frac{\langle [I - \langle I \rangle]^2 \rangle}{\langle I \rangle^2} = \frac{I_{inc}^2}{I_{co}^2} \equiv K^{-2} \quad (5.6)$$

where $I_{co}$and $I_{inc}$are the coherent and incoherent components of the total signal intensity indicated in Fig. 3.

Dependence of *K*-factor of fading versus the signal intensity scintillationσ_I^2, was fully discussed in [14, 15]. For our numerical analysis presented below we notice that the range $\langle \sigma_I^2 \rangle$of the scintillation index variations, from 0.4 to 0.8, was obtained from numerous experimental trials of the troposphere at heights till 1-2 km, where relations between this parameter and the refractivity of the turbulence in the irregular atmosphere taken into account [8-14]. Thus, from experiments described there, it was estimated refraction index power variations around $C_n^2 \approx 10^{-15}$ $m^{-2/3}$ and around $C_n^2 \approx 10^{-13}$ $m^{-2/3}$, for nocturnal and daily periods, respectively. As also was shown in [14, 15], in the cases of mean and strong atmospheric turbulences occurring in the irregular atmosphere, the index of signal intensity scintillations varies from 0.4 to 0.9. If so, it is easy can be found from (5.6) that the corresponding *K*-parameter of fast fading varies in the range of about 1.1 to 1.6.

It indicates the existence of direct visibility (i.e., the LOS component) between both terminals, the optical source and the optical detector, accompanied by the additional effects of multipath phenomena (i.e., NLOS multipath component) caused by multiple scattering of optical rays at the turbulent structures, formed in the perturbed atmospheric regions, observed experimentally [6-10, 14, 15]. In such scenarios, where $\langle \sigma_I^2 \rangle$ = 0.7-0.9 the *K*-factor, described multipath fading phenomenon within the atmospheric wireless propagation channel, changes around the unit. Having now information about *K*-factor, we can predict deviations of the data stream parameters in the multipath channels passing through the strong turbulences occur in the irregular atmosphere.

Thus, the capacity or spectral efficiency described versus *K*-factor by Eq. (5.4) and (5.5), respectively, can be easy estimated for various scenarios occurring in the atmospheric channel and for different conditions of the inner noise of the optical transmitters and receivers inside the optical communication under consideration. One of the examples seen in Fig. 7, for different additive signal-to-noise ratios (SNRs) and for a "point" optical receiver (with respect to the diameter of the detector).

We take the *K*-parameter much wider, varying in the interval from 0.1 to 30, that is, to cover the “worst” case, when *K*<<1, which describes by Rayleigh law [15] passing the quasi-LOS case, when $K \approx 1$, and finally achieving situation where *K*>>1 (ideal LOS case in propagation, described by Delta-shape Gaussian law). As can be seen, in the strong perturbed irregular atmosphere (with strong turbulences), where$K \leq 1$, the spectral efficiency is around of 0.7-0.8 (for all SNRs) and for *K*>3-5 (weak turbulence) it is around 1.5-2.5 (for SNR=5, 10, 15, and 20dB).

The next, usually used in informatics science parameter, is a bit-error-rate (BER) which describe loss of information bits in signal data stream passing irregular atmosphere consisting various kinds of turbulences – from weak and small to strong and large [14, 15].

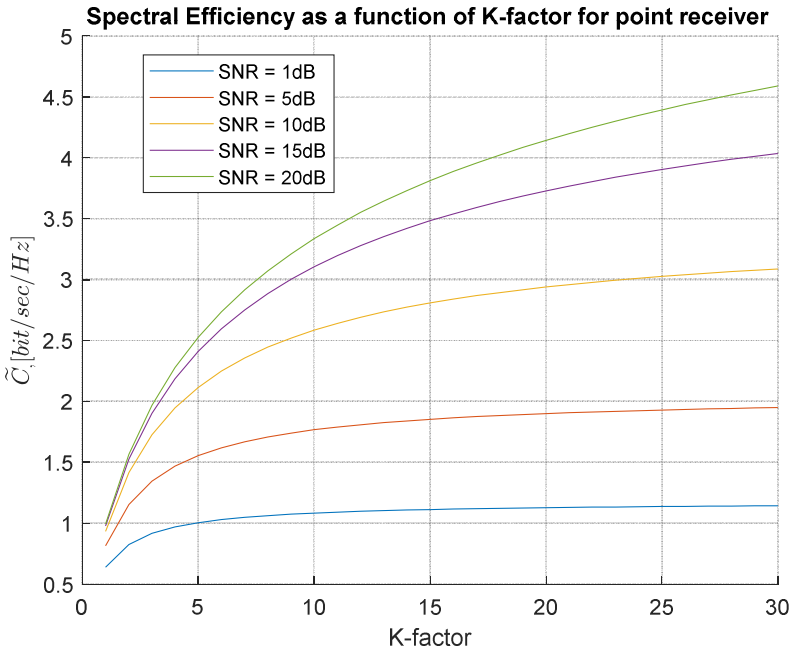

Fig. 7. Spectral efficiency vs. *K*-factor for *SNR* = 1, 5, 10, 16 dB for point receiver. Range between the terminals is *L* = 1 km.

The parameter of data stream, *BER*, versus K-factor for various values of additive (Gaussian) *SNR* is presented in Figs. 8a,b for signal variance of 2 dB and 5 dB, described weak turbulence conditions and strong turbulence conditions, respectively, occurring in daily Mediterranean atmosphere.

As seen from Figs. 8a and 8b, strong turbulence atmospheric conditions, defined by $K<<1$, result in relatively greater bit-error-rate (achieving for a constant SNR 0.1-0.25) comparing to weak turbulence effects with $K > 2$ (achieving for constant SNR values less than 0.01 with further saturation at BER close to zero for all, small and large values of SNR). As was expected with increase of SNR inside the optical wireless link, this saturation and limitation of BER to zero takes place faster.

Therefore, "reaction" of the turbulence on optical signal propagation inside wireless atmospheric links plays a major role in fading effects, caused by turbulence [10, 14, 15]. Therefore, there are subjects of particular interest for estimation of optical communication parameters, such as *BER* and *SNR* and prediction of maximal losses, caused by strong turbulence.

Next, we analyze effects of fading (e.g., the changes of the *K*-parameter) on bit-error-rate (*BER*) conditions within the turbulent wireless communication link consisting weak and strong turbulences.

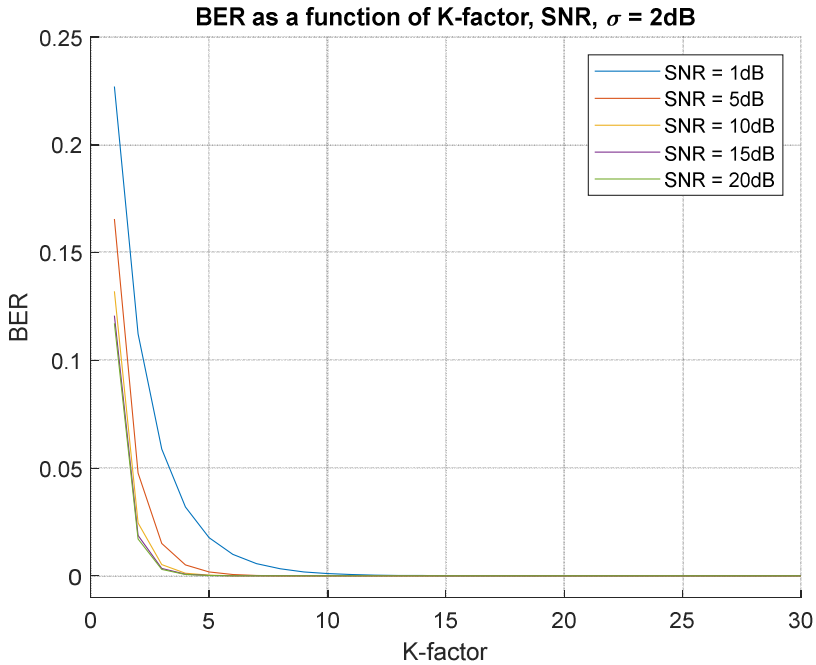

Fig. 8a. BER vs. K-factor for the additive (Gaussian) SNR changed from 1 dB (worst case) to 20 dB (good case) for signal intensity variations of 2 dB.

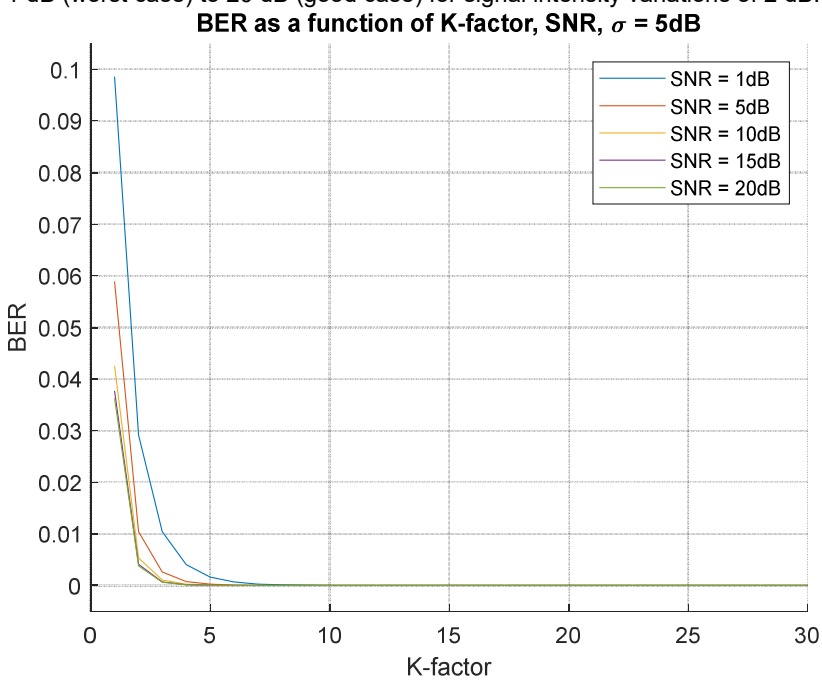

Fig. 8b. The same, as in Fig. 8a, but for signal variations of 5 dB.

As shown in [8-12], depending on what kind of turbulence, moderate (with $\langle C_n^2 \rangle = 5 \cdot 10^{-14}$) occurring at altitudes up to 100-200m, or weak (with $\langle C_n^2 \rangle = 4 \cdot 10^{-16}$) occurring at altitudes of 1-2 km, the effects of fading become stronger (at the first case) and weaker (at the second case). In other words, at higher atmospheric altitudes for the horizontal atmospheric channels, where the LOS component exceeds the multipath (NLOS) component (i.e., for *K*>1), the *BER*-characteristic becomes negligible and can be ignored as well as other fading characteristics in design of land-atmospheric or pure atmospheric links.

Finally, in [14, 15] an optimal algorithm for minimization of the BER of optical bandpass signals was proposed for different situations occurring in optical atmospheric communication links. Thus, taking some measured data, presented in [8-10, 14], we can show here some examples. In our computations, we used the following parameters of the channel and measured data: $\sigma = 2dB$, and $SNR_{add} = 1dB$. The results of the computations are shown in Fig. 9 for *BER* as a function of the fading parameter *K* obtained from the experimental data [8-10].

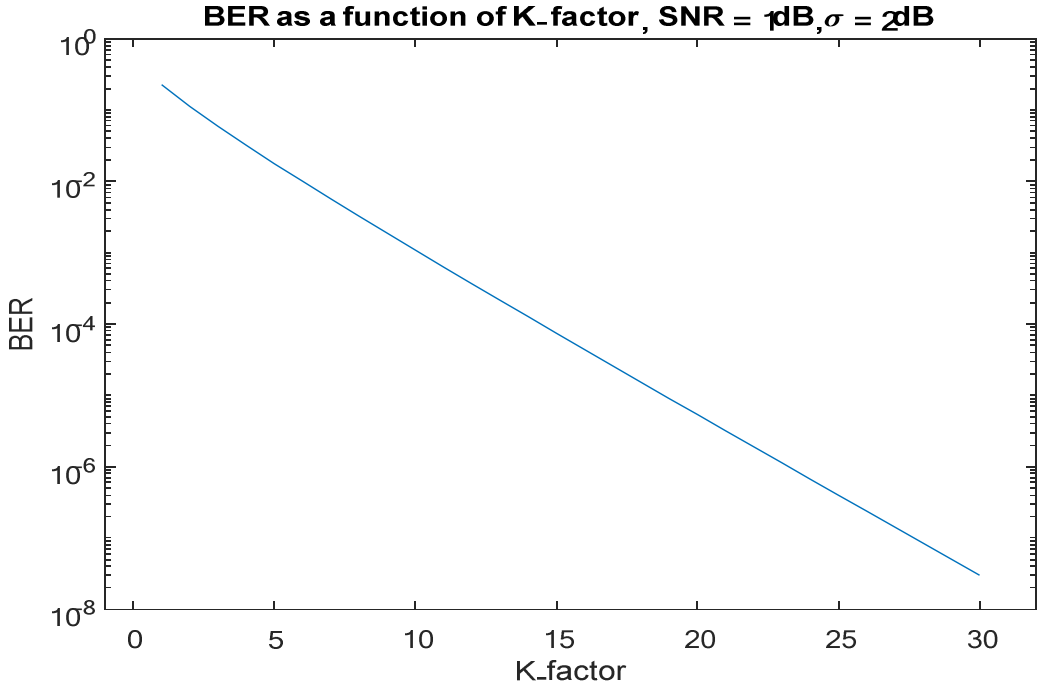

Fig.9. BER as a function of *K*.

As seen from Fig. 9 with increase of *K* parameter; that is, when LOS component becomes predominant with respect to NLOS multipath components, it is found that BER decreases essentially from 10^{-2} for $K \approx 5$ to 10^{-6} for $K \approx 20$ (i.e., for the atmospheric link at altitudes of 100-500 m filled by turbulent structures [8-13]).

At the same time, as was expected in [14, 15], the spectral efficiency found to increase with *K*-parameter. Hence, with the increase of the spectral efficiency of the data stream (from 0.8 to 1.0), it was found also a simultaneous sharp decrease of

BER. To show this, we present in Fig. 10 the dependence of BER versus the spectral efficiency.

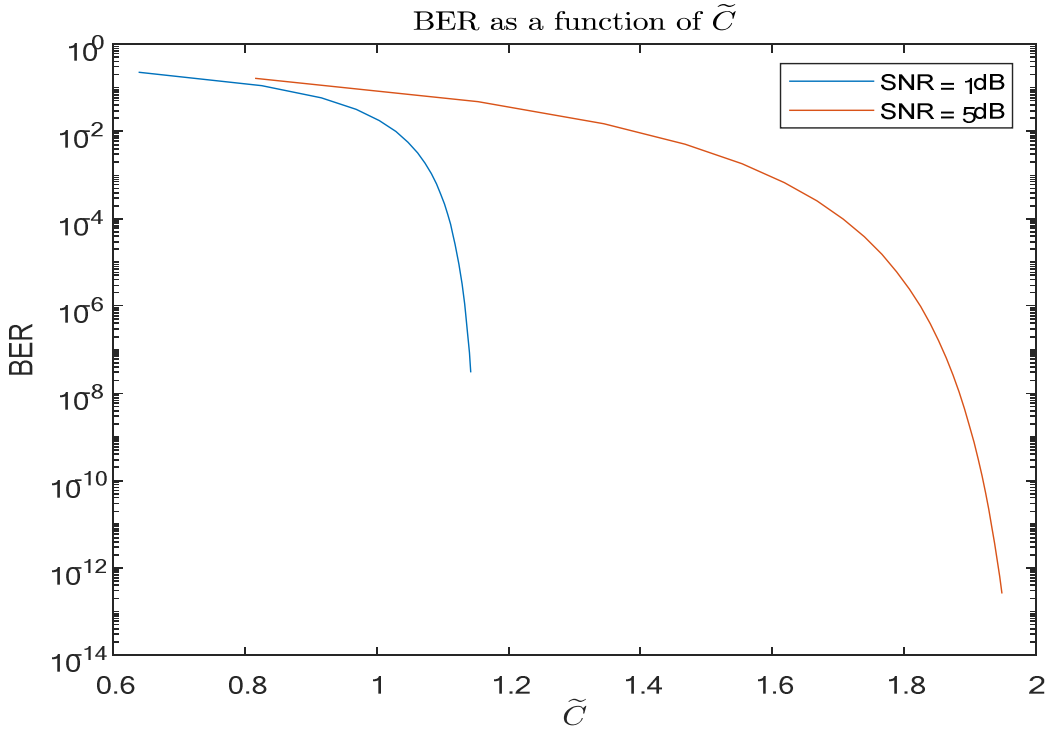

Fig. 10. BER vs. spectral efficiency$\tilde{C}$.

As can be seen, for small $\tilde{C} = C/B_{\omega}$, BER is sufficiently high. At the range $\tilde{C} = 0.6 - 0.7$, as a real range of *K*-factor in the turbulent atmosphere, the BER is twice smaller compared with the previous case, but it is high enough to loss information inside the channel with fading occurring during the effects of turbulence. It should be noted that, and as was discussed above and follows from illustrations of Fig. 8, the increase of SNR inside the channel (from 1*dB* to 5*dB*) cannot decrease BER significantly even for high spectral efficiency. Generally speaking, with increase of the spectral efficiency from 0.1 to 0.7, the *BER* parameter decreases approximately in three times.

At the same time, as noted in [14, 15] and is seen from Fig. 7, the spectral efficiency also increases with increase of fading parameter *K*. Thus, increase of $\tilde{C} = C/B_{\omega}$ from 0.2 to 0.8 leads to sharp decrease of BER from 0.3-0.5 to 0.003–0.005, the effect, which depends on SNR in the optical channel and additionally decreases with increase of SNR.

Summary

In this work, we have analyzed the effects of turbulent gaseous structures, small-scale, moderate-scale, and large-scale, weak and strong, on signal data, which pass via atmospheric communication links with fading. Where analyzed the

effects of structure parameter of the refractive index deviations on the index of scintillation of the optical signal passing atmospheric channels with fading. Relations between these parameters are investigated both for conditions of weak gaseous turbulences, moderate and strong turbulences observing experimentally in the middle–latitude troposphere. Analytically and numerically was obtained the relation between signal intensity deviations, called the scintillation index, usually used during analysis of optical atmospheric communication links, and the well-known Rician K-parameter of fast fading, usually used during analysis of radio wireless communication channels to unify both approached for description of tropospheric optical communication links with fading. Additionally was analyzed analytically the effects of tropospheric scattering on intensity loss of and its impact in fast fading phenomena occurring in atmospheric links in conditions of non-line-of-sight (NLOS). Finally, using relation between the fading Rician K-factor and scintillation index, were analyzed data stream parameters, such as capacity, spectral efficiency and bit-error-rate (BER) for predicting of quality of service (QoS) accounting for the effects of weak, moderate and strong gaseous turbulent structures filled atmospheric channels with fading. The latter aspect is very important for designers of land-atmospheric and atmospheric-atmospheric optical communication links related to the corresponding optical networks beyond 5G.

Bibliography

1.Kolmogorov, A. N., "The local structure of turbulence in incompressible viscous fluids for very large Reynolds numbers", in *Turbulence, Classic Papers on Statistical Theory*, S. K. Friedlander and L. Topper, Eds., pp. 151-155, Wiley-InterScience, New York, 1961.

2.Tatarskii, V.I., *The Effects of the Turbulent Atmosphere on Wave Propagation*, Trans. For NOAA by the Israel Program for Scientific Translations, Jerusalem, 1971.

3.Kraichman, R. H., "On Kolmogorov's inertial-range theories", *J. Fluid Mech*., vol. 62, pp. 305-330, 1974.

4.Ishimaru, A., *Wave Propagation and Scattering in Random Media* , Academic Press, New York, 1978.

5.Andrews, L. C., and Phillips, R. L., *Laser Beam Propagation through Random Media*, 2nd Ed., SPIE Press, Bellingham, WA, USA, 2005..

6.Samelsohn, G. M., "Effect of inhomogeneities' evolution on time correlation and power spectrum of intensity fluctuations of the wave propagating in a turbulent medium", *Soviet Journal on Communic. Technol. Electron*., vol. 38. Pp. 207-212, 1993.

7.Samelsohn, G. M., and B. Ya. Frezinskii, *Propagation of Millimeter and Optical Waves in a Turbulent Atmosphere*, St.-Petersburg: Telecommunication University Press, 1992.

8.Bendersky, S., N. Kopeika, and N. Blaustein, "Prediction and modeling of line-of-sight bending near ground level for long atmospheric paths", *Proc. of SPIE Int. Conf.,* San Dieg, August 3-8, 2004, pp. 512-522.

9.Bendersky, S., N. Kopeika, and N. Blaustein, "Atmospheric optical turbulence over land in middle east coastal environments: prediction, modeling and measurements", J. Applied Optics, vol. 43, pp. 4070-4079, 2004.

10.Blaunstein, N., and N. Kopeika (Eds.), *Optical Waves and Laser Beams in the Irregular Atmosphere*, Boca Raton, FL: CRC Press, Taylor and Frances Group. 2018.

11.Bello, P. A., "A troposcatter channel model", *IEEE Transactions on Communications*, vol. 17, pp. 130-137, 1969/

12.Stremler, F. G., *Introduction to Communication Systems*, Addison-Wesley Reading, 1982.

13.Champagne, F. H., C. A. Friehe, J. C. LaRye, and J. C. Wyngaard, "Flux measurements, flux-estimation techniques, and fine-scale turbulence measurements in the unstable surface layer over land", *J. Atmospheric Science*, vol. 34, pp. 515-530, 1977.

14.Blaunstein, N., Sh. Arnon, A. Zilberman, and N. Kopeika, *Applied Aspects of Optical Communication and LIDAR*, New York: CRC Press, Taylor &Francis Group, 2010.

15.Blaunstein, N., and Ch. Christodoulou, *Radio Propagation and Adaptive Antennas for Wireless Communication Links: Terrestrial, Atmospheric and Ionospheric*, Wiley InterScience, NJ, 2007.